ADSORPTION OF 5′-AMP AND CATALYTIC SYNTHESIS OF 5′-ADP ONTO PHOSPHATE SURFACES: CORRELATION TO SOLID MATRIX STRUCTURES

ANA CLAUDIA TESSIS[1],* HÉLIO SALIM DE AMORIM[2], MARCOS FARINA[3], FERNANDO DE SOUZA-BARROS[2] and ADALBERTO VIEYRA[1,**]

[1]*Department of Biochemistry, Institute of Biomedical Sciences,* [2]*Department of Solid State Physics, Institute of Physics, and* [3]*Institute of Biophysics Carlos Chagas Filho, Federal University of Rio de Janeiro, Rio de Janeiro 21941–590, Brazil*

(Received November 9, 1993)

Abstract. A non-enzymatic formation of 5′-ADP starting from phosphorylation of 5′-AMP in the presence of either calcium phosphate or calcium pyrophosphate precipitates is reported. This reaction is taken as a model for the study of heterogeneous catalysis of transphosphorylation in prebiotic conditions. Experiments were performed in completely aqueous media and in media containing dimethyl sulfoxide (Me_2SO), to simulate periods of dehydration in primitive aquatic environments. It has been observed that the nucleotide is adsorbed onto both calcium phosphate and calcium pyrophosphate in accordance with Langmuir isotherms. Adsorptive capacity and affinity of the precipitates for nucleotide are changed by the presence of Me_2SO, suggesting that the interaction between biomonomers and surfaces can be modulated by the degree of hydration of the anionic components of these compounds. In completely aqueous environments, formation of 5′-ADP from 5′-AMP adsorbed on precipitates of calcium phosphate and calcium pyrophosphate is very small. However, in the presence of 60% Me_2SO this synthesis increases by factors of 3 and 6 for surfaces of calcium phosphate and calcium pyrophosphate, respectively, and follows first-order kinetics. Determinations of free energy changes show that phosphorylation of 5′-AMP adsorbed to these precipitates is thermodynamically favorable. Depending on the precipitation time of the samples and the composition of the medium, structural analysis of these precipitates by electron and X-ray diffraction shows changes in their cristallinity grade. It is proposed that these changes are responsible for the modulation of the quantity of adsorbed nucleotides to the surface of solid matrices as well as the catalytic activity of the precipitates.

Abbreviations: 5′-AMP – 5′-adenosine monophosphate; 5′-ADP – 5′-adenosine diphosphate; BTP – 1,3-bis[tris(hydroxymethyl)-methylamino]propane; CTEM – conventional transmission electron microscopy; Tris – tris(hydroxymethyl)aminomethane; Pi ($H_2PO_4^-/HPO_4^{2-}$) – orthophosphate; Pi.Ca – calcium phosphate; PPi ($H_3P_2O_7^-/H_2P_2O_7^{2-}$) – pyrophosphate; PPi.Ca – calcium pyrophosphate; EGTA – [ethylenebis(oxyethylene)nitrilo]tetraacetic acid

1. Introduction

Bernal (1951) was the first to propose a catalytic role of minerals during the process of chemical evolution. Clays, iron hydroxides, and insoluble phosphates may have acted as catalysts of biomolecular synthesis in primitive aqueous environments (Ponnamperuma *et al.*, 1982; Ferris *et al.*, 1988; Hermes-Lima and Vieyra,

* This work has been submitted to the Department of Biochemistry, Institute of Biomedical Sciences, UFRJ, by A.C.T. in partial fulfillment of requirements for the MS degree.

** To whom correspondence should be addressed.

Origins of Life and Evolution of the Biosphere **25:** 351–373, 1995.

1989, 1992). An increase in concentration of dilute monomer solutions (such as the nucleotide 5′-AMP) by adsorption on mineral surfaces could represent the first step in condensation and transphosphorylation reactions that could permit the appearance of both non-informational and informational replicating molecular systems (Orgel, 1992). Several authors (Miller and Parris, 1964; Lohrmann and Orgel, 1971; Rao *et al.*, 1980; Acevedo and Orgel, 1986) developed models showing that energy donor molecules and self-replicating systems must have formed, interconverted, and evolved by passing through repeated drying and wetting cycles during which concentration onto mineral surfaces occurred (Lahav and Chang, 1976, 1982).

5′-ADP is one of the nucleotides that has been synthesized in potentially prebiotic conditions. Several years ago, Ponnamperuma *et al.* (1963) reported the formation of 5′-ADP from 5′-AMP and ethyl metaphosphate by the action of ultraviolet light. More recently, 5′-ADP was obtained using pyrophosphate (PPi) as phosphorylating agent in the presence of apatite crystals (Neuman *et al.*, 1970). The aim of the present work was to study the formation of 5′-ADP from phosphorylation of 5′-AMP by calcium phosphate (Pi.Ca) or calcium pyrophosphate (PPi.Ca) surfaces as a model for prebiotic catalysis of condensing phosphorylation reactions. This study aimed to correlate the structure of these solid matrices – specifically their composition and crystalline degree – with their adsorptive and catalytic properties.

2. Experimental

2.1. Materials

5′-AMP (free acid), pyrophosphate (PPi) (tetrasodium salt), Bis-Tris Propane buffer (BTP), Tris buffer, and the reagents used in the measurement of synthesized 5′-ADP (P-enolpyruvate, NADH, EGTA, pyruvate kinase and lactate dehydrogenase) were purchased from Sigma Chemical Company (St. Louis, MO). The $CaCl_2.2H_2O$ salt was supplied by E. Merck (Darmstadt, Germany), and the phosphoric acid was from Carlo Erba (Italy). The radioactive orthophosphate (^{32}Pi) – obtained from the Nuclear and Energy Research Institute (São Paulo, Brazil) – was purified using the method of Boyer and Bryan (1967). Deionized glass-distilled water was used in the preparation of the solutions. All other chemicals used were of analytical grade.

2.2. Methods

Precipitates of Pi.Ca (or PPi.Ca) were prepared by rapidly mixing 14 μl of 0.5 M Pi (Tris salt) (or 35 μl of 0.2 M PPi, sodium salt) and 20 μl of 1.0 M $CaCl_2$ (neutralized to pH 8.0 with BTP buffer) into 0.9 ml of a 0.22 M BTP.HCl solution. To prevent formation of large aggregates in the solid matrix, the tubes were vigorously vortexed for 5–10 s and left to precipitate for 30 min at room temperature (about 25 °C) with

periodic shaking. High buffer concentrations were used in order to limit pH changes to less than 0.1 units during precipitation.

Adsorption of 5′-AMP to the pre-formed Pi.Ca or PPi.Ca precipitates was started by the addition of 5′-AMP in a final volume of 1.0 ml at 37 °C. To measure the amount of adsorbed 5′-AMP the tubes were centrifuged at 4000 × *g* for 20 min (Hermes-Lima *et al.*, 1990), and an aliquot of each supernatant was diluted to 1.0 ml with deionized water. The absorbance was measured at 259 nm using a molar extinction coefficient of 15.4×10^3 M^{-1} (Morell and Bock, 1954). The amount of adsorbed nucleotide was calculated from the difference between the absorbance measured in the supernatants and that corresponding to an initial control solution without Pi (or PPi) precipitates.

5′-ADP formation was measured spectrophotometrically by using the coupled enzyme system pyruvate kinase and lactate dehydrogenase, and recording the oxidation of NADH to NAD^+ at 340 nm, using a molar extinction coefficient of 6.22×10^3 M^{-1} (Morell and Bock, 1954). Briefly, 0.2 ml-samples were removed under vigorous stirring from the incubation media and mixed with 0.8 ml of a solution containing 40 mM EGTA (to dissolve the precipitate), 50 mM Tris-HCl (pH 7.4), 25 mM $MgCl_2$, 100 mM KCl, 1 mM P-enolpyruvate, 0.1 mM NADH, 4.9 units of pyruvate kinase, and 7 units of lactate dehydrogenase. The amount of 5′-ADP synthesized was calculated from the difference in absorbance before and 10 min after addition of the enzymes.

For Ca/P molar-ratio determinations, the Pi.Ca solid matrix was prepared using either $^{45}CaCl_2$ and nonradioactive Pi, or nonradioactive $CaCl_2$ and ^{32}Pi. Tubes containing 1.0 ml of reaction mixture were stirred vigorously by vortexing, and a 0.1 ml aliquot was immediately removed and counted in a liquid scintillation counter. The suspension was then centrifuged at 4000 × *g* for 20 min and another 0.1 ml of the clear solution from the top of the tube was counted. Ca and Pi fractions present as insoluble complexes were calculated from the difference between the radioactivity present in the supernatant and the total radioactivity in the mixture. The amount of PPi present in the PPi.Ca solid matrix was measured after centrifugation of samples. Precipitates were dissolved in 1 M HCl and incubated for 24 h at 37 °C. The Pi resulting from the acid hydrolysis of PPi was measured by a slight modification of the method of Fiske and SubbaRow (1925). Briefly, aliquots of 0.05 ml were diluted with distilled water to 1.0 ml, and then mixed with 0.4 ml of ammonium molybdate and 0.2 ml of reducer solution containing 1-amino-2-naphthol-4-sulfonic acid, sodium sulfite, and sodium bisulfite. After 15 min at room temperature, absorbance was recorded at 660 nm.

Structural analysis of the Pi.Ca and PPi.Ca precipitates was carried out using conventional transmission electron microscopy (CTEM), X-ray and electron diffraction techniques. For these studies, solid phase matrices were prepared by diluting 3.5 ml of Pi (Tris salt) (or 8.75 ml of PPi, sodium salt) and 4.0 ml of 1 M $CaCl_2$ into 250 ml of a 50 mM BTP.HCl solution. During precipitation the pH of the solution was continuously monitored, and maintained at pH 8.0 by microliter additions of

HCl or NaOH. The suspension was shaken during 1 h at room temperature allowing complete formation of Pi.Ca and PPi.Ca precipitates. For CTEM observations and electron diffraction studies, a drop with the precipitates was touched with a formvar carbon coated grid and immediately dried. The microscope used was a Zeiss CEM 902, operating in both the elastic bright field and elastic diffraction modes. For X-ray analysis the suspension was centrifuged and the precipitate was lyophilized. X-ray diffractograms were obtained at room temperature with a Cobalt-tube (λ = 1.8 Å) of a type F Siemens apparatus. The electron and X-ray diffraction lines from these precipitates do not show significant contributions from systems other than Pi.Ca and PPi.Ca. Finally, it should be mentioned that the structural characteristics of the samples in Me_2SO-containing media were the same regardless of whether the samples lyophilized (X-ray diffraction) or air-dried (electron diffraction). The electron diffraction of PPi.Ca samples prepared with Me_2SO (Figure 12B) did not change during the period of observation under CTEM. We conclude that the residual Me_2SO expelled by the electron beam during the time required for obtaining the electron micrographs must have been negligible.

3. Results

3.1. Adsorption of 5′-AMP onto precipitated calcium phosphate and calcium pyrophosphate

Figure 1A shows the adsorption isotherm of 5′-AMP onto precipitated Pi.Ca (at pH 8.0) in the absence or in the presence of 80% Me_2SO. The adsorptive capacity (i.e., the maximum amount of 5′-AMP adsorbed for a given amount of Pi solid, and calculated from the adsorption isotherm described by Equation 1 below) was 850 and 2230 nmol of adsorbed 5′-AMP in 1 ml medium (152 and 343 nmol of adsorbed 5′-AMP per μmol of solid Pi) in the absence and in the presence of Me_2SO, respectively. In both cases, i.e., in totally aqueous media and in the presence of Me_2SO, the adsorption of 5′-AMP onto precipitated Pi.Ca can be described by a Langmuir isotherm (Langmuir, 1918):

$$AMP_{ad} = [AMP].K_{ad}.AMP_{max}/([AMP].K_{ad} + 1) \quad (1)$$

where $[AMP]$ is the equilibrium concentration of 5′-AMP, K_{ad} is the adsorption coefficient, and AMP_{max} is the surface adsorption capacity for 5′-AMP (Ferris and Hagan, 1986; Hermes-Lima and Vieyra, 1989; Hermes-Lima *et al.*, 1990).

Figures 1B and 1C show the AMP_{max} and K_{ad} values, respectively, for the adsorption isotherms of 5′-AMP onto precipitated calcium phosphate at different Me_2SO concentrations (0 to 80%). It can be observed that one of the effects of Me_2SO on the adsorption of 5′-AMP is to give rise to a biphasic profile, an effect that may reflect changes in the structure of the solid matrix (see below). It can be seen that the surface adsorption capacity for 5′-AMP decreases and the affinity

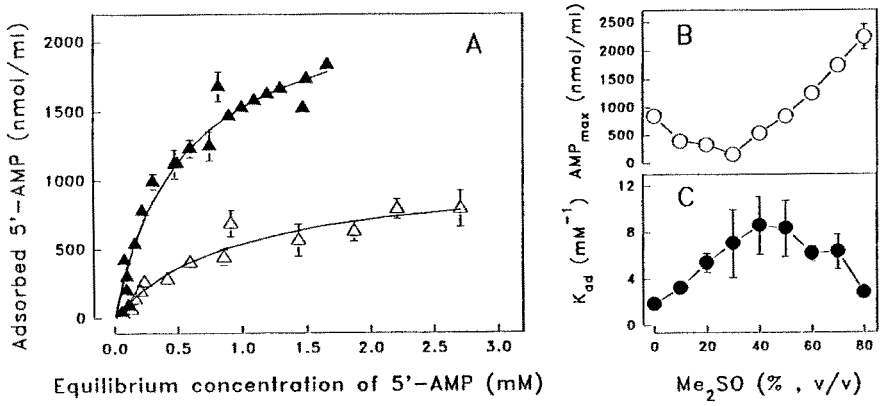

Fig. 1. A: Adsorption isotherm of 5′-AMP onto solid calcium phosphate in the absence (△) or in the presence of 80% Me_2SO (▲). Assays containing 0.2 M BTP buffer (pH 8.0), 7 mM Pi (Tris salt) and 20 mM $CaCl_2$ were incubated at room temperature (25 °C) for 30 min to allow formation of a solid phase of calcium phosphate. Once the formation was achieved, the following initial concentrations of 5′-AMP (in mM): 0.1, 0.2, 0.3, 0.4, 0.5, 0.7, 1.0, 1.3, 1.6, 2.0, 2.5, 3.0, and 3.5 were added. The samples were then incubated for 3 h at 37 °C. The amount of adsorbed 5′-AMP was plotted as a function of the equilibrium 5′-AMP concentration (added 5′-AMP *minus* adsorbed 5′-AMP). B and C: Parameters of the adsorption isotherm of 5′-AMP onto solid calcium phosphate (AMP_{max} and K_{ad}) as a function of Me_2SO concentrations. They were obtained employing the Langmuir equation (see text). Statistical analysis (t test) shows that there are differences ($P < 0.05$) in K_{ad} values between the groups with 0% and 40% Me_2SO, and the groups with 40% and 80% Me_2SO. Conversely, there is no statistical difference between the groups with 0% and 80% Me_2SO.

increases in the range of 0 to 40% Me_2SO. On the other hand, for concentrations above 40% Me_2SO the AMP_{max} increases, attaining – at 80% Me_2SO – a value twice that obtained for the adsorption isotherm in totally aqueous media, whereas the surface affinity for the nucleotide decreases.

The Ca/P molar ratio in the solid matrix of Pi.Ca is the same – for both the totally aqueous medium and in media with different Me_2SO concentrations (data not shown) – indicating that this solvent does not affect the composition of the precipitate. On the other hand, structural analysis of the Pi.Ca precipitate by small-angle X-ray scattering (Figure 2) shows that in the presence of 60% Me_2SO there is a reduction of the scattering intensity by a factor of 4.5. This reduction corresponds to a decrease in the average Pi.Ca particle size, suggesting a dispersing action of the co-solvent on the particles, probably related to its high dipole moment (Parker, 1961, 1962) and the consequent modification in the dielectric constant of the medium (Travers and Douzou, 1974). The net result should be an increase of the effective adsorptive area of the precipitate. The increase in AMP_{max} caused by Me_2SO can in part be explained by this effect.

In totally aqueous media no 5′-AMP adsorption is observed with PPi.Ca precipitate. The nucleotide adsorption is measurable only with Me_2SO concentrations

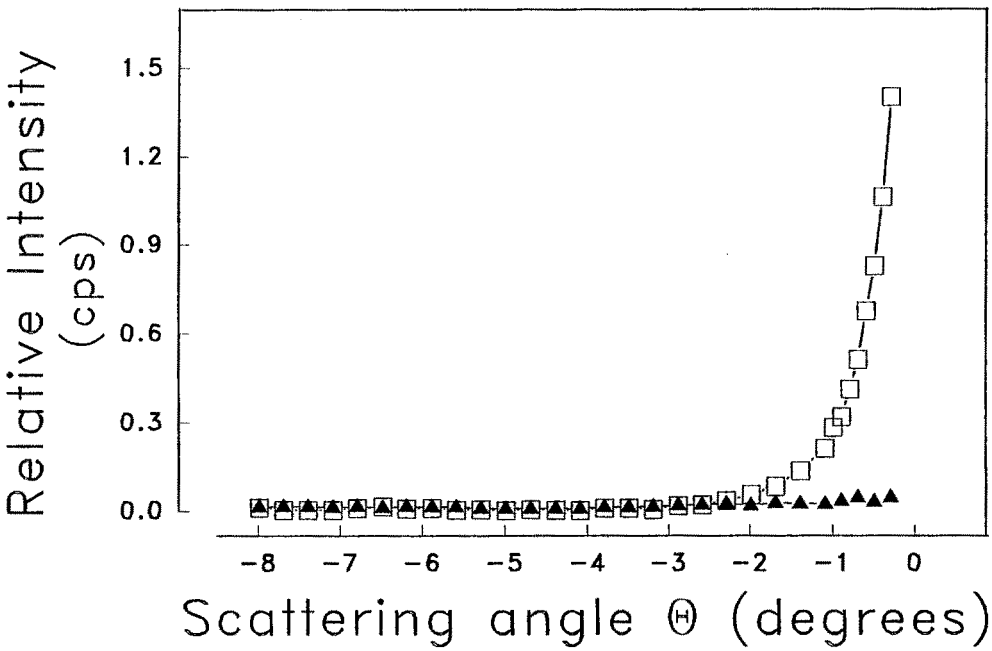

Fig. 2. Small angle X-ray scattering of calcium phosphate samples in the absence (□) or in the presence (▲) of 60% Me_2SO. Samples contained 50 mM BTP buffer (pH 8.0), 20 mM $CaCl_2$, and 7 mM Pi (Tris salt). In both cases, after the formation of a solid phase of calcium phosphate (30 min at room temperature) the samples were centrifuged and the precipitates placed in 1 mm capillary tubes. The relative scattering intensity is plotted as a function of the scattering angle θ of the Copper X-ray radiation (λ = 1.5 Å). The factor 4.5 (see text) is obtained when one compares the ratio of the areas under the experimental points in the absence and in the presence of Me_2SO.

above 40%. Figure 3A shows the adsorption isotherm of 5′-AMP onto precipitated PPi.Ca in the presence of 80% Me_2SO. As in the case of Pi.Ca, the adsorption can be described by a Langmuir isotherm (Equation 1). The calculated values of AMP_{max} and K_{ad} are shown in Figure 3B and 3C, respectively. The Ca/P molar ratio in the solid matrix of PPi.Ca is the same in a totally aqueous medium and in the presence of different Me_2SO concentrations (data not shown). Finally, evidence for the same dispersing effect of the co-solvent can also be suggested for PPi.Ca precipitate giving rise to an increase of its total surface area.

3.2. Time course of 5′-ADP formation from 5′-AMP adsorbed onto precipitated calcium phosphate and calcium pyrophosphate

When 2 μmol/ml of 5′-AMP is incubated at pH 8.0 for 12 days at 37 °C in totally aqueous media in the presence of either Pi.Ca or PPi.Ca precipitates, 6.2 and 5.4 nmol 5′-ADP/ml are synthesized, respectively (see below Table II). In

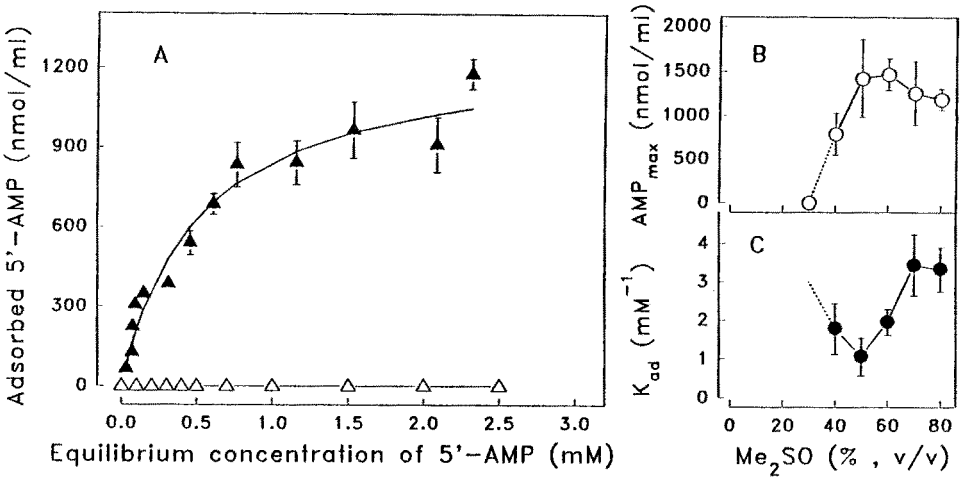

Fig. 3. A: Adsorption isotherm of 5′-AMP onto solid calcium pyrophosphate in the absence (△) or in the presence of 80% Me_2SO (▲). Assays were as indicated in Figure 1, except that 7 mM PPi (sodium salt) was used instead of Pi (Tris salt). B and C: Parameters of the adsorption isotherm of 5′-AMP onto solid calcium pyrophosphate obtained employing the Langmuir equation (see text).

the absence of calcium (orthophosphoric acid neutralized with Tris), and therefore without solid matrix, the formation of 5′-ADP from 7 mM Pi and 2 mM 5′-AMP is barely detectable. In the presence of 7 mM PPi (again with no calcium) only 2.6 nmol 5′-ADP/ml is formed. Based on the previously shown adsorptive properties of the Pi.Ca and PPi.Ca precipitates (Figures 1 and 3), these results suggest that their surfaces can promote phosphorylation of 5′-AMP, forming the phosphoanhydride bond of the synthesized 5′-ADP molecule.

Figure 4 shows the time course of 5′-ADP formation from adsorbed 5′-AMP onto both Pi.Ca and PPi.Ca precipitates in the presence of 60% Me_2SO. In the presence of calcium – i.e., with formation of a solid matrix – 17.2 and 31.6 nmol 5′-ADP/ml are synthesized with Pi and PPi, respectively (empty and filled circles in Figure 4). When this experiment is repeated in the absence of calcium, the results are as follows: a) in the presence of 7 mM Pi, the formation of 5′-ADP cannot be detected; b) with 7 mM PPi, 4.2 nmol 5′-ADP/ml is synthesized (filled triangles in Figure 4). The formation of 5′-ADP – in the presence and absence of precipitates – follows pseudo first-order kinetics:

$$ADP_t = ADP_{max}(1 - e^{-kt}) \quad (2)$$

where ADP_t is the amount of ADP formed at a given time, ADP_{max} characterizes the amount synthesized at the steady-state plateau, and k is the pseudo first-order rate constant of synthesis. The k values for all the experimental conditions described in Figure 4 are shown in Table I.

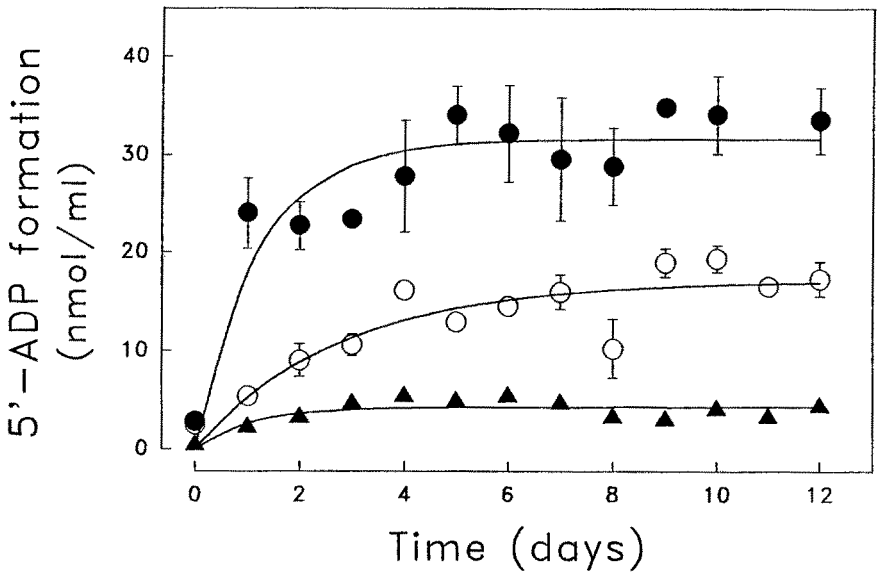

Fig. 4. Time course of 5′-ADP formation in precipitates of calcium phosphate and calcium pyrophosphate in the presence of 60% Me_2SO. Assays containing 0.2 M BTP buffer (pH 8.0), 20 mM $CaCl_2$, 7 mM Pi (Tris salt) (o) or PPi (sodium salt) (•), and 5 mM sodium azide were incubated at room temperature for 30 min to allow the formation of a solid phase of calcium phosphate or calcium pyrophosphate. Once formed, the assays were supplied with 2.0 mM 5′-AMP and placed at 37 °C. ▲: Assays without solid phase. The 5′-ADP formed was measured as indicated under Materials and Methods. The pseudo first-order rate constants of 5′-ADP formation were calculated using Equation 2 (see text).

TABLE I

Pseudo first-order rate constant of 5′-ADP formation with different phosphorylating agents[a]

Phosphorylating agent[b]	Cation	$k(h^{-1})$[c]
$PPi_{(aq)}$	–	4.04×10^{-2}
$Pi_{(s)}$	Ca^{2+}	1.50×10^{-2}
$PPi_{(s)}$	Ca^{2+}	3.45×10^{-2}

[a] Assays were as indicated in the legend of Figure 4.
[b] The subscripts (aq) and (s) mean completely soluble form and solid form, respectively.
[c] The k values were calculated using Equation 2 (see text).

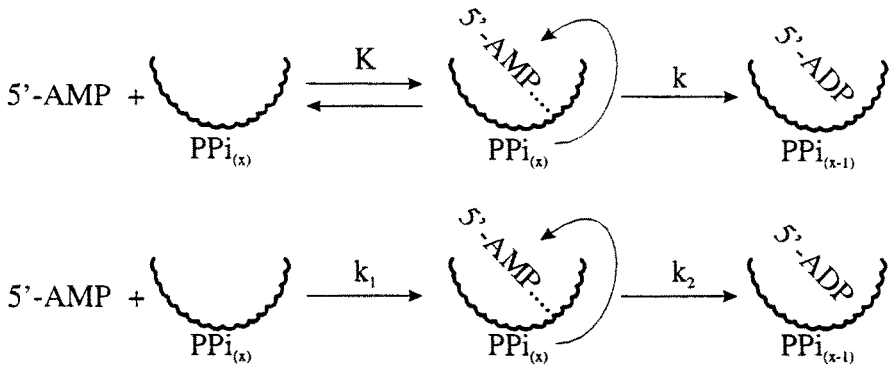

Fig. 5. Representation of 5′-AMP binding and phosphorylation at a site in PPi.Ca precipitates ($PPi_{(x)}$). In the upper scheme the formation of a complex between the biomonomer and the site (with a dissociation constant K), is the rate-limiting step of the overall reaction. In the lower scheme, k_2 (the 'catalytic constant' of transphosphorylation) is much lower than k_1 (the rate constant of binding). The subscript (x) is the number of PPi molecules in each site.

Since the synthesis of 5′-ADP follows the same kinetics either in an homogeneous phase (without precipitates) or in the presence of a solid matrix, it can be postulated that there is a similar chemical path for the transphosphorylation reaction. However, the fact that the rate constants for 5′-ADP formation in the presence of PPi are of the same order of magnitude for both the homogeneous phase (i.e. with very diluted reagents) or in the presence of solid matrix – where the 5′-AMP is adsorbed on its surface (Figures 1 and 3) – indicates that the reaction in solid phase is slower than would be expected if 5′-AMP had become more concentrated. As depicted in the scheme shown in Figure 5, this could be due to either a) formation of a complex between the solid matrix having catalytic properties and the mononucleotide, as in the case of enzyme-substrate complex formed in the active site of the enzymes; or b) change in the rate-limiting step of the overall reaction, from the formation of the bimolecular complex to the formation of the P-O-P bond of the 5′-ADP molecule. Both mechanisms could occur in the solid matrix of old minerals like Pi and PPi, and could have been preserved during evolution. These alternatives can be found in contemporaneous catalysts, such as proteins with enzymatic activity (Jencks, 1969).

3.3. THERMODYNAMIC PARAMETERS OF THE 5′-ADP FORMATION IN PRECIPITATED CALCIUM PHOSPHATE AND CALCIUM PYROPHOSPHATE

In purely aqueous media the formation of a phosphoanhydride bond such as the linkage between the α and β phosphoryl groups of the 5′-ADP molecule, is an

TABLE II

Free energy variation of non-enzymatic 5′-ADP formation from 5′-AMP (equilibrium reached at 12 days)[a]

Reaction	Medium	5′-ADP yield (nmol/ml)	$\Delta G^{0\prime}$ (kcal/mol)[b]	ΔG (kcal/mol)[c]
5′-AMP + Pi	Water	6.2	+8.59	−1.13
5′-AMP + Pi	Me_2SO	17.2	+8.15	−1.58
5′-AMP + PPi	Water	5.4	+5.98	−0.11
5′-AMP + PPi	Me_2SO	31.6	+5.62	−0.47

[a] Assays were as indicated in the legend of Figure 4.
[b] The $\Delta G^{0\prime}$ values were calculated from the quantities of 5′-AMP adsorbed, 5′-ADP formed and Pi or PPi precipitated, employing the Equation: $\Delta G^{0\prime} = -RT \ln K_{eq}$.
[c] ΔG were calculated from the $\Delta G^{0\prime}$ values and the initial concentrations of reagents and products.

endergonic process with $\Delta G^{0\prime}$ ranging 7 to 10 kcal/mol, depending on medium composition (Atkinson, 1977; Flodgaard and Fleron, 1974; de Meis, 1993). Figure 4 shows that 4 nmol 5′-ADP/ml are formed from 5′-AMP and soluble PPi (without calcium in the media, i.e., without solid matrix) indicating that the PPi can phosphorylate the nucleotide – in the absence of enzymatic catalysts – in a near equilibrium reaction ($\Delta G \approx 0$). The 5′-ADP synthesis from 5′-AMP and PPi represents one example of a reaction involving one precursor biomonomer (5′-AMP) and one condensing molecule, in this case PPi (Hulshof and Ponnamperuma, 1976; Ferris and Hagan, 1984), which has been proposed as one of the primitive energy donors before the appearance of ATP (Kulaev *et al.*, 1980; Baltscheffsky *et al.*, 1986).

However, the adsorbed 5′-AMP can also be phosphorylated by Pi in the presence of calcium, i.e., in the absence of a conventional energy donor substrate with greater free energy of hydrolysis. Free energy variations associated with the formation of 5′-ADP were calculated from the quantities formed from the amount of 5′-AMP adsorbed onto Pi.Ca surfaces (Table II). Although the $\Delta G^{0\prime}$ value for the formation of 5′-ADP in the Pi.Ca solid matrix is essentially the same as that calculated for aqueous solutions (Atkinson, 1977; de Meis, 1993), it can be observed in Table II that the reaction free energy is slightly negative and, therefore, that the synthesis of 5′-ADP becomes thermodynamically favorable. This observation suggests a unique role for adsorption phenomena, that of increasing the reactants concentrations in microenvironments, allowing the surfaces to participate actively in chemical reactions during evolution (Rao *et al.*, 1980; Ponnamperuma *et al.*, 1982; Ferris *et al.*, 1989). In the primitive diluted aqueous media (Ponnamperuma *et al.*, 1982; Orgel, 1988), the formation of a solid matrix with a potential phosphorylating capacity could have changed the direction of phosphorylation reactions, thus facilitating the

spontaneous occurrence of processes that are thermodynamically unfavorable in homogeneous phase.

As can be seen in Figure 1B, the quantities of 5′-AMP adsorbed onto Pi.Ca precipitates are essentially the same in the absence or in the presence of 60% Me_2SO. The solvent also did not affect the amount of precipitate formed per unit volume of suspension (Section 3.1). However, the yield of 5′-ADP synthesis in the presence of Me_2SO is 2 to 3 times higher than in the absence of the solvent (Figure 4; Table II). These last results indicate that in the equilibrium conditions the increase in the level of 5′-ADP formed does not depend only on a mass effect. The solvent could favor the synthesis reaction by changing the structural characteristics of the precipitate and, consequently, the physical nature of the interactions between Pi and the α-phosphoryl group of the 5′-AMP molecule. From an evolutionary point of view, another interesting possibility can be inferred from these Me_2SO results. As proposed by Cairns-Smith (1982) for clays, highly dipolar molecules could have intercalated between the prebiotic phosphate surfaces and the nucleotide, thus favoring the transphosphorylation in a water-deficient environment. For example, it has been reported that ethylene glycol can substitute for water molecules on Ca^{2+}-montmorillonite – forming structures with a high level of organization (Reynolds, 1965) – and that the addition of this type of solvent (Me_2SO, ethylene glycol) in contemporary energy-transducing enzymes can favor phosphorylation reactions that are thermodynamically unfavorable in totally aqueous media (de Meis, 1993). This type of interaction between dipolar molecules and mineral surfaces with catalytic properties may have been an earlier acquisition – preserved during chemical evolution. Later, this feature could have been incorporated into catalytic systems that co-evolved after the emergence of life (Baltscheffsky *et al.*, 1986; Erskelens, 1990; Hermes-Lima e Vieyra, 1992; Vieyra *et al.*, 1994).

The PPi.Ca precipitate phosphorylates 5′-AMP with a $\Delta G^{0'}$ that is 2 to 2.5 kcal/mol smaller than the calculated value for Pi.Ca (Table II). This difference corresponds to the $\Delta G^{0'}$ value of hydrolysis of PPi in the same conditions (Flodgaard and Fleron, 1974; de Meis, 1993) suggesting that solid matrices of PPi are also able to couple thermodynamically two reactions with opposite $\Delta G^{0'}$ (synthesis of 5′-ADP and hydrolysis of PPi). The same coupling is seen with some contemporaneous enzymatic systems in crucial metabolic pathways (Lipmann, 1941; Atkinson, 1977).

3.4. Correlation between the structures of precipitated calcium phosphate and calcium pyrophosphate and their adsorptive capacity

5′-AMP adsorption isotherms were analyzed both for Pi.Ca precipitates of recent formation (30 min) and those preserved for several days at room temperature. Substantial differences in the adsorption parameters were found. In the case

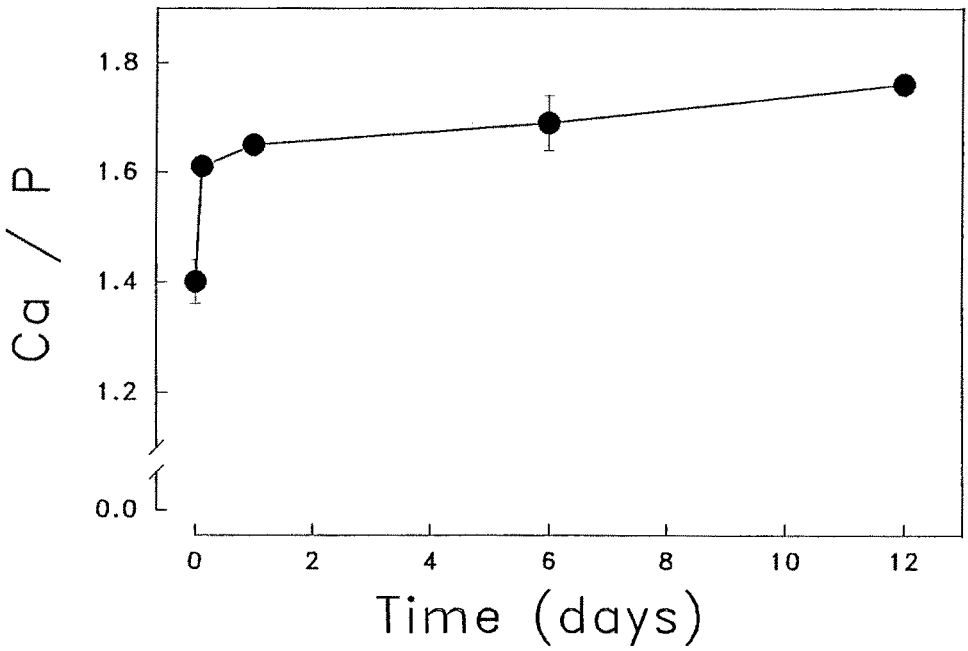

Fig. 6. Ca/P ratio as a function of calcium phosphate precipitation time. Samples contained 0.2 M BTP buffer (pH 8.0), 20 mM $CaCl_2$, 7 mM Pi (Tris salt), and 5 mM sodium azide. Precipitation times are indicated on the *abscissa*. The ratios were measured as indicated under Materials and Methods.

of recently formed precipitates, the adsorption capacity (AMP_{max}) of the surface was 2260 nmol/ml and the adsorption coefficient (K_{ad}) was 0.18 mM^{-1} ($1/K_{ad}$ = 5.6 mM). With precipitates preserved for 15 days, the adsorption capacity decreases (AMP_{max} = 690 nmol/ml) and the affinity of the surface for 5′-AMP increases (K_{ad} = 0.64 mM^{-1}; $1/K_{ad}$ = 1.6 mM). These results suggest the occurrence of changes in the structure of the precipitates. These time-dependent structural changes might be related to the occurrence of changes in the interaction between nucleotide and the surface of precipitates. Structural modifications in meta-stable calcium phosphate compounds have already been observed (van Kemenade and Bruyn, 1987). At early stages an amorphous and meta-stable compound is formed, which eventually undergoes phase transformations resulting in more stable and crystalline forms, including hydroxyapatite, depending on the pH of the medium (Miller and Parris, 1964; van Kemenade and Bruyn, 1987). It could be postulated that, if repeated in cyclical and reversible conditions (Lahav and Chang, 1976), these changes could have caused fluctuations in the adsorption of monomers in primitive aqueous environments and in the condensation reactions involving such monomers during chemical evolution (Oró, 1976).

The above transformations manifest themselves, among other ways, as changes in the Ca/P ratio of precipitate structures (van Kemenade and Bruyn, 1987). For Pi.Ca sample it is observed as an increase in the Ca/P ratio as a function of the time during which the mineral remained in suspension at room temperature (Figure 6). This increase was more pronounced in the first 24 hours. The Ca/P values of 1.40 for 30 min and 1.65 for 24 h of precipitation correspond to octacalcium phosphate and hydroxyapatite, respectively (van Kemenade and Bruyn, 1987).

To ascertain modifications in the degree of crystallization, X-ray diffraction analyses were conducted in samples corresponding to precipitation times of 30 min, 3 h and 24 h (Figure 7). The diffractograms show the structural evolution of this precipitate. It exhibits a not well defined phase at 30 min, the appearance of peaks at 3 h, and the narrowing of these peaks after 24 h. These results indicate that the Pi.Ca structure undergoes a gradual transformation from a state with strong amorphous character to another with some degree of crystallization. A comparison of the peak intensities and of their positions in the diffractogram with those of standard samples shows that the crystalline precipitate could be either octacalcium phosphate or hydroxyapatite. For these solid matrices, there is great similarity between the diffraction spectra of the two compounds (Taves, 1963). It might be that the precipitate is a mixture of different phosphates, probably with predominance of octacalcium phosphate in early stages, since it grows faster than hydroxyapatite, although the latter is more stable (Brown *et al.*, 1962).

Transmission electron microscopy of 15-day-old Pi.Ca precipitates shows the presence of small crystalline grains forming aggregates (Figure 8A). Electron diffraction analysis of these samples confirmed the existence of the crystalline phase (Figure 8B). Moreover, inspection of the interplanar distances is in agreement with the X-ray diffraction analysis.

Figure 9 shows the X-ray diffractogram of a PPi.Ca sample after 15 days of precipitation. The presence of sharp peaks indicates a well defined crystalline structure. Transmission electron microscopy of these PPi.Ca samples (Figure 10A) shows that they are constituted of much larger monocrystals than those observed in Pi.Ca (compare with Figure 8A). Indeed, electron diffraction (Figure 10B) indicates that the observed region contains a monocrystal (arrow in Figure 10A).

3.5. THE PRECIPITATION OF CALCIUM PHOSPHATE AND CALCIUM PYROPHOSPHATE IN ME_2SO: MODIFICATIONS IN THEIR ADSORPTIVE AND PHOSPHORYLATING CAPACITIES

Figures 1B, 3B and 4 and Table II show that the adsorptive and phosphorylating properties of Pi.Ca and PPi.Ca precipitates, particularly those of pyrophosphates, present significant changes after the addition of Me_2SO to the water medium. The following experiments were carried out to analyze the structural changes of these precipitates induced by the co-solvent, and to correlate these changes with those observed in their catalytic properties. They show that the effect of Me_2SO on the

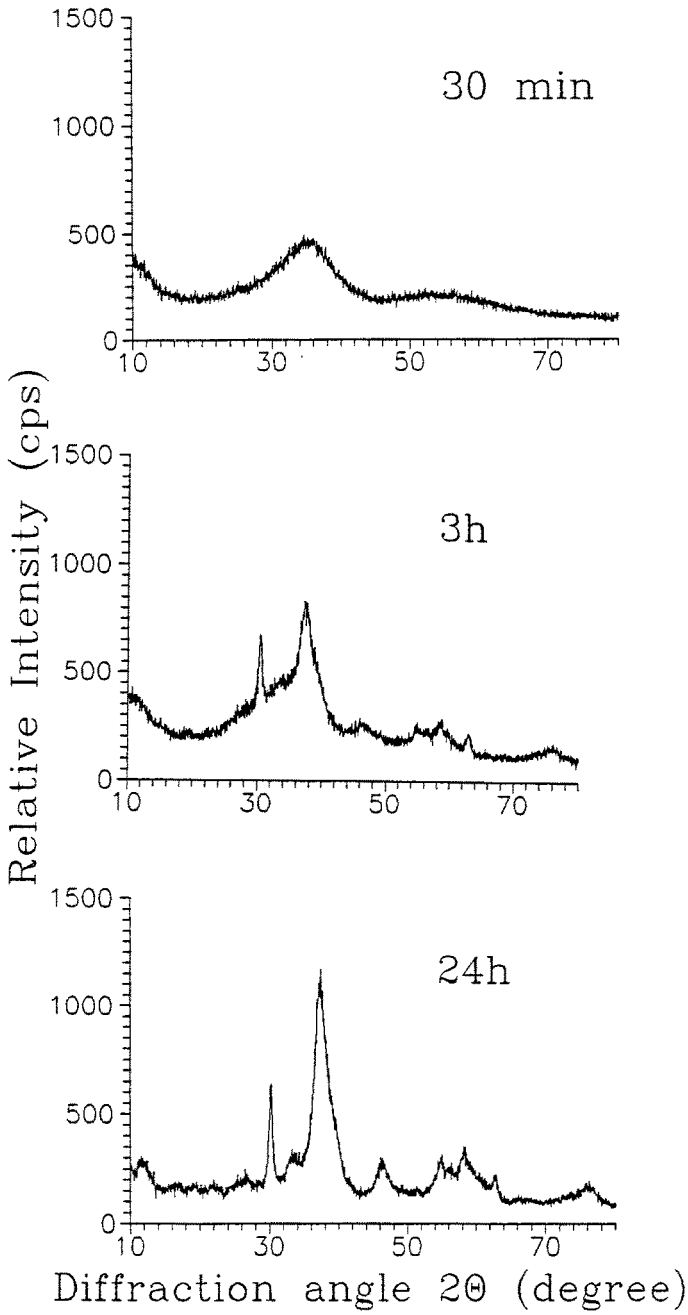

Fig. 7. X-ray diffraction of samples of calcium phosphate obtained at different precipitation times. Samples contained 50 mM BTP buffer (pH 8.0), 20 mM $CaCl_2$, 7 mM Pi (Tris salt), and 5 mM sodium azide. After the formation of a solid phase of calcium phosphate at 30 min, 3 h and 24 h, the samples were centrifuged, the precipitates were lyophilized, and X-ray diffraction analysis were performed as indicated under Materials and Methods.

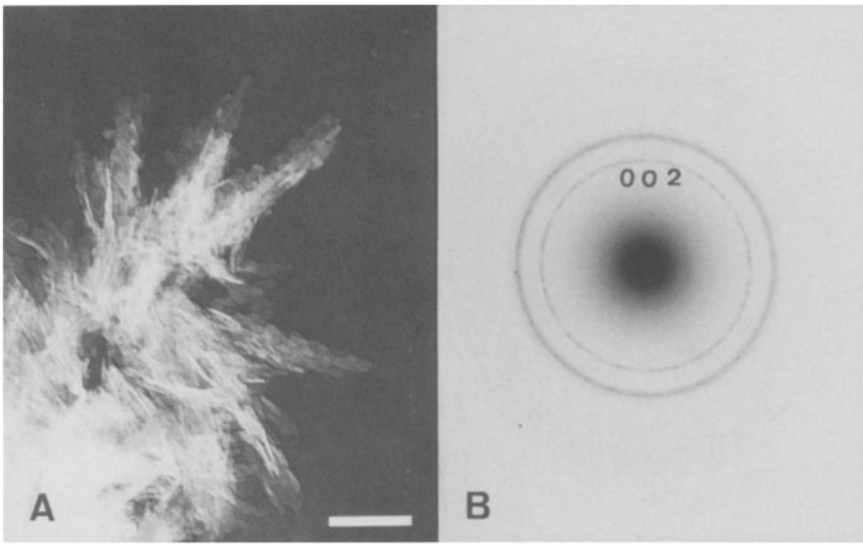

Fig. 8. Transmission electron microscopy (A) and electron diffraction (B) of calcium phosphate precipitates. Assays were as indicated in the legend of Figure 7. After the calcium phosphate precipitation (15 days at room temperature) the samples were analyzed by electron microscopy, as indicated under Materials and Methods. Bar in Figure 8A represents 1.0 μm. The (002) lattice planes indicated in Figure 8B correspond to those of octacalcium phosphate and hydroxyapatite (see text).

solid matrices of Pi and PPi salts, in contrast to what was previously proposed (Hermes-Lima and Vieyra, 1992), is more than one of simple dehydration.

Figure 11A shows a CTEM image of Pi.Ca after 15 days of precipitation in the presence of 60% Me_2SO. As in the Pi.Ca samples formed in completely aqueous medium (Figure 8A), the presence of crystalline grains is also observed. Moreover – and contrasting with the results obtained for PPi.Ca (compare Figures 10 and 12, below) – the addition of 60% Me_2SO does not produce significant changes in the crystalline pattern of Pi.Ca, as concluded from the observation of the diffraction patterns shown in Figures 8B and 11B. This may be the cause for the small effect of this Me_2SO concentration in the adsorption of 5′-AMP (an increase of about 40%; see Figure 1B). On the other hand, the Me_2SO-induced increase in the phosphorylating capacity of the Pi.Ca matrix is more than two times lower than that observed in PPi.Ca (compare yields in Table II). The differences in adsorption and 5′-ADP synthesis observed for Pi.Ca in water and 60% Me_2SO (Figure 1B and Table II) may be associated with the differences in aggregation of the grains

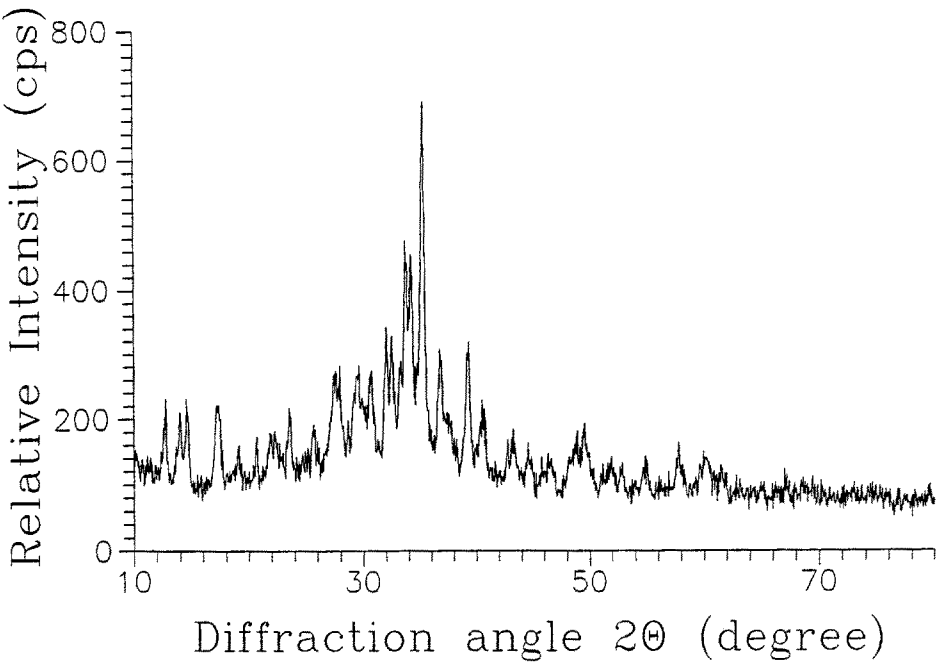

Fig. 9. X-ray diffraction of calcium pyrophosphate precipitates. Samples contained 50 mM BTP buffer (pH 8.0), 20 mM $CaCl_2$, 7 mM PPi (sodium salt), and 5 mM sodium azide. After the formation of a solid phase (15 days at room temperature) the samples were centrifuged, the precipitates were lyophilized, and X-ray diffraction analysis were performed as indicated under Materials and Methods.

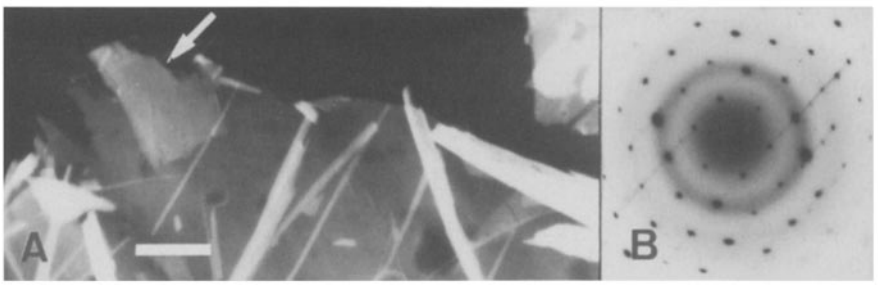

Fig. 10. Transmission electron microscopy (A) and electron diffraction (B) of calcium pyrophosphate precipitates. Assays were as indicated in the legend of Figure 9. After precipitation (15 days at room temperature) the samples were analyzed by electron microscopy as indicated under Materials and Methods. Bar in Figure 10A represents 10 μm. The single crystal diffraction pattern in Figure 10B comes from the crystal indicated by the arrow in Figure 10A.

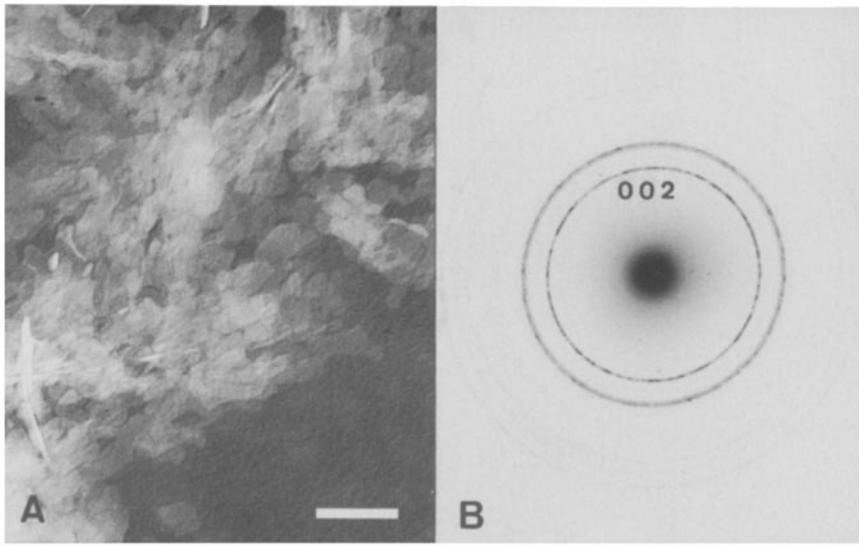

Fig. 11. Transmission electron microscopy (A) and electron diffraction (B) of calcium phosphate in the presence of 60% Me_2SO. Assays were as indicated in the legend of Figure 7, except that 60% Me_2SO (v/v) was added. After precipitation (15 days at room temperature) the samples were analyzed by electron microscopy as indicated under Materials and Methods. Bar in Figure 11A represents 0.1 μm. The (002) lattice planes indicated in Figure 11B, correspond to those of octacalcium phosphate and hydroxyapatite (see text).

(Figures 8A and 11A), which would cause a change in the total available area for binding and catalysis.

In the case of PPi.Ca formed in the presence of Me_2SO, the images obtained by CTEM show aggregation of very small particles (principal panel of Figure 12). The addition of 60% Me_2SO results in no electron diffraction pattern, even after incubation for 15 days (inset of Figure 12), indicating that crystallization does not occur or that the crystalline phase is too small relative to the amorphous one. A comparison of the CTEM image and electron diffraction pattern of these samples (Figure 12) with those of PPi.Ca formed in water (Figure 10), confirms that there exists a considerable reduction in their crystallization. The X-ray diffraction of these samples also confirms the low crystallization in the presence of Me_2SO (data not shown).

Finally, it is of interest to note that in completely aqueous medium, where PPi.Ca shows a well defined crystalline structure (Figures 9 and 10), the phosphorylating capacity of the precipitate is very low (2.6 nmol 5′-ADP/ml). Conversely, the amorphous matrix of PPi.Ca formed in Me_2SO-containing medium (Figure 12) catalyzes the synthesis of 31.6 nmol 5′-ADP/ml (Figure 4, filled circles; Table II). Therefore, the decrease in the degree of crystallinity appears to be clearly related

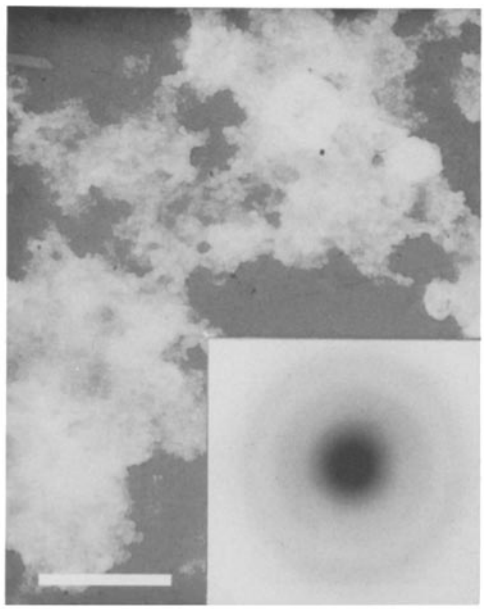

Fig. 12. Transmission electron microscopy (principal panel) and electron diffraction (inset) of calcium pyrophosphate samples in the presence of 60% Me_2SO. Assays were as indicated in the legend of Figure 9, except that 60% Me_2SO (v/v) was added. After precipitation (15 days at room temperature) the samples were analyzed by electron microscopy as indicated under Materials and Methods. Bar in the principal panel represents 0.5 μm. Inset shows a typical diffraction pattern of the precipitates indicating that they are amorphous.

with the more than ten-fold increase in the phosphorylating capacity of the PPi.Ca matrix.

4. Discussion and Conclusions

The results reported in this paper show that the surfaces of phosphate and pyrophosphate precipitates, adsorbing 5′-AMP as anion-exchangers, (Gibbs *et al.*, 1980) are capable of reacting with the phosphoryl group of the adsorbed 5′-AMP leading to the synthesis of 5′-ADP (Figures 1, 3, and 4). The present observations indicate that the surfaces not only provide the phosphoryl group but also catalyze the formation of a phosphoanhydride linkage, in analogy with those catalyzed by contemporary energy-transducing enzymes (Pickart and Jencks, 1984; Pedersen and Carafoli, 1987; Hermes-Lima and Vieyra, 1992; Vieyra *et al.*, 1994). Figures 6 to 12 show evidence of variable crystalline states in these precipitates. These variations could be used in a model for processes depending on reversible 'amorphous $\leftrightarrow$ crystalline' transitions in primitive epochs. For instance, these transitions could

have been capable of modulating adsorptive and catalytic phenomena involving biomonomers.

It is possible to postulate that progress along a specific line of molecular complexity increased through various states of

activation→condensation→blocking→blocking–release→activation

if polymerization from activated monomers during chemical evolution had catalytic support from mineral surfaces with properties modified by cyclic environmental changes (Cairns-Smith and Davis, 1977; Stillinger and Wassermann, 1978; Cairns-Smith, 1982). Through their influence on those steps, cyclic environmental changes would have modulated the rhythm and the specificity of the formation of new and more complex molecular structures. In addition, if localized defects in ancestral minerals had trapped primitive molecules, allowing their interaction with other molecules (Plaçon and Tchoubar, 1977), changes in the chemical composition of these minerals, in the crystalline lattice itself, and/or in the magnitude of the prevalent attractive and repulsive forces, could have contributed to direct and modulate synthetic reactions during chemical evolution.

'Hydration-dehydration' cycles seem to have had a relevant role during chemical evolution, modulating the adsorption of molecules in the catalysts present in primitive aqueous media (Bernal, 1951; Lahav and Chang, 1976, 1982; Hermes-Lima and Vieyra, 1989, 1992). It is likely that this modulation could have been enhanced through structural changes of ancient minerals. In particular, the formation of amorphous phases rich in localized defects could be induced by these cycles. In this manner, modifications in the binding of molecules onto clays, gypsum, phosphates, and other minerals, would have been caused not only by fluctuations in pH, ionic strength and temperature, but also by reversible changes in the mineral structure itself (Burton *et al.*, 1969; Chan *et al.*, 1987; Orenberg *et al.*, 1985; Hermes-Lima *et al.*, 1990).

The synthesis of 5′-ADP onto Pi.Ca and PPi.Ca is a thermodynamically favorable reaction (Table II) due to the concentration of the reactants (precipitation of phosphate or pyrophosphate plus adsorption of the nucleotide). The PPi.Ca precipitate appears to be able to couple two reactions: the endergonic synthesis of 5′-ADP and the exergonic hydrolysis of PPi in water (de Meis, 1993). Energy coupling in phosphoryl transfer reactions is a crucial property of contemporary energy-transducing systems (Lipmann, 1941; Jencks, 1969; Atkinson, 1977; Pickart and Jencks, 1984), and it may be speculated that this property appeared early during evolution, after the formation of phosphate minerals with catalytic activity (Hermes-Lima and Vieyra, 1992; Vieyra *et al.*, 1994). Figure 13 depicts hypothetical reaction cycles of phosphorylation involving these ancient catalysts and 5′-AMP, a biomonomer synthesized in potentially prebiotic conditions (Ponnamperuma and Mack, 1965; Neuman *et al.*, 1970; Yamagata *et al.*, 1982).

The fact that the $\Delta G^{0'}$ values of the reactions of synthesis of 5′-ADP with Pi and PPi as phosphorylating agents (Table II) are similar to those found in aqueous

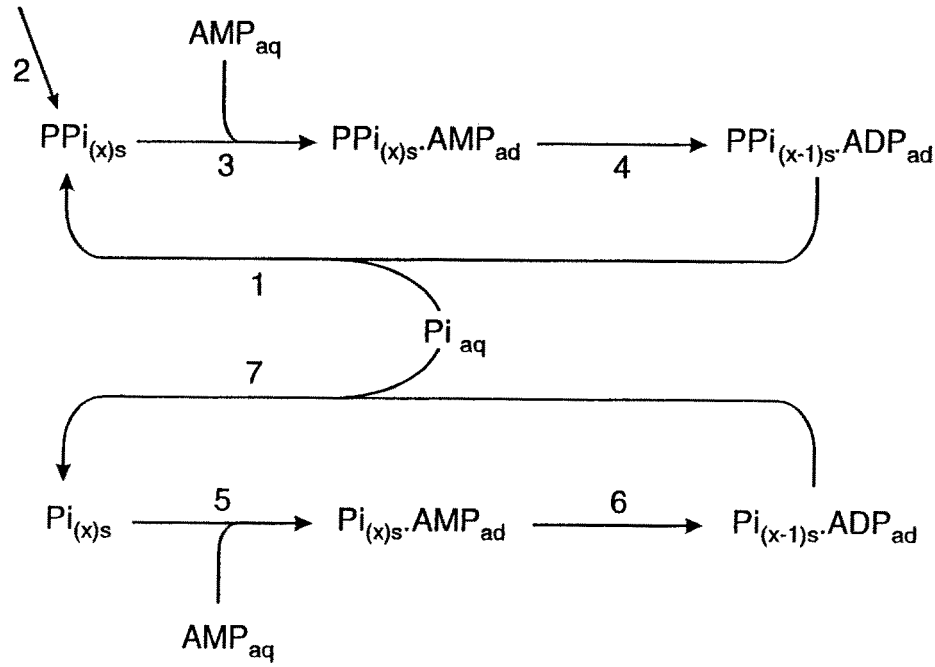

Fig. 13. Hypothetical prebiotic phosphorylation cycles of 5′-AMP to 5′-ADP by precipitated PPi or Pi. Solid pyrophosphate ($PPi_{(x)s}$; where 'x' is the number of PPi molecules in the precipitate) could have been formed by condensation of orthophosphate (Pi) present in primitive aqueous environments in mild (Hermes-Lima, 1990a) or drastic conditions (Yamagata *et al.*, 1991) (step 1). Alternatively, it could have been synthesized by phosphorolysis of compounds present on primitive Earth (Miller and Parris, 1964; Ferris, 1968; Vieyra *et al.*, 1994) (step 2). Then, the precipitated PPi could have adsorbed the biomonomer 5′-AMP (step 3), later phosphorylated by the matrix to 5′-ADP (step 4). The lower sequence represents the adsorption of aqueous 5′-AMP onto precipitated Pi (step 5), followed by transphosphorylation to 5′-ADP (step 6) and regeneration of the solid matrix through precipitation of soluble Pi salts (step 7). The model does not consider the existence of phase transitions, such as those shown in Figures 6 to 12. For clarity, the Ca^{2+} ions are not represented, although the net charge of the surface should have been positive (Wächtershäuser, 1988, Hermes-Lima *et al.*, 1990).

solution (Floodgaard and Fleron, 1974; Atkinson, 1977; de Meis, 1993), suggests that this kind of mineral would not be able to change the equilibrium between reactants and products. This is in contrast to what happens in the active center of energy-transducing enzymes, probably due to the fact that minerals are not fully competent to exclude the water from their surfaces. In F_0F_1 ATP synthases of mitochondria and chloroplasts, in pyrophosphatases, and in ion-motive ATPases, the P-O-P bond of their respective ligands is of low energy whenever they are present in the hydrophobic catalytic site ($K_{eq} \approx 1$; $\Delta G^0 \approx 0$), shifting to values

of high free energy of hydrolysis ($K_{eq} \gg 1$; $\Delta G^0 \ll 0$) only after the transfer of those compounds to an aqueous medium (de Meis, 1993). Although the boundary of precipitated minerals could be in contact with water, it can be assumed that in hydrophobic niches of minerals such as clays present in an ancient aqueous scenario (Ferris and Hagan, 1986; Ferris *et al.*, 1989), the nucleotides derived from more primitive structures, the soluble Pi – coming from the water medium – and the divalent cations, could have found an appropriate shelter to react. In these microenvironments with restricted access of water, dipolar aprotic substances of potential prebiotic interest (Oró, 1976; Cairns-Smith, 1982; Hermes-Lima and Vieyra, 1992) could also be stored. Among the latter, some are capable of desolvating anions (Parker, 1961, 1962), and for this reason phosphoryl transfer reactions would have K_{eq} close to 1 (de Meis, 1993).

The specific properties of mineral sites that are capable of producing variations in K_{eq}, could have been incorporated and later improved by more complex energy-transducing systems (Cairns-Smith, 1982; Hermes-Lima and Vieyra, 1992; Vieyra *et al.*, 1994). The results obtained with Me_2SO are in line with the proposal that molecules with a large dipole moment such as urea, formamide and hydrazine (Oró, 1976; Cairns-Smith, 1982), may have coadjuvated in the regulation of phosphorylation reactions. This could have occurred through interferences in the adsorption of the reactants and also through structural changes in the solid matrix. The contrasting differences between the effects of Me_2SO in the phosphate and pyrophosphate structures as depicted in the electron diffraction patterns of Figures 11 and 12 inset (compare with 8B and 10B in pure water), lead to the conclusion that such dipole molecules could have had different effects depending on the existence of specific chemical bonds (the phophoanhydride linkage, for instance) in minerals of the same origin (Hermes-Lima, 1990).

Although minerals in solid phase lack the flexibility of contemporary enzymes (Erskelens, 1990; Hermes-Lima and Vieyra, 1992), they could have been one of the alternatives for catalysis before the appearance of polynucleotides. This possible function of minerals could have been taken over by primitive catalysts of the RNA type and, finally, by protein catalysts in later periods of evolution (Cairns-Smith, 1982; Hermes-Lima *et al.*, 1990; Hermes-Lima and Vieyra, 1992; Vieyra *et al.*, 1994). Mineral modifications that can be brought about by variations of pH, temperature, concentration and species of divalent cations present, and water activity in reversible cycles of hydration-dehydration (Bernal, 1951; Lahav and Chang, 1976, 1982; Hermes-Lima and Vieyra, 1989, 1992), could have given the appropriate flexibility to the catalysts that acted on Earth during the billion-years period of chemical evolution.

Acknowledgments

This research was supported by grants from FUJB/UFRJ, FAPERJ, CNPq and FINEP (Brazil). We acknowledge Prof. L. Q. de Amaral (University of São Paulo) for helping with the small-angle X-ray scattering experiments. We also thank Dr. Martha Sorenson for critical reading of the manuscript.

References

Acevedo, O. L. and Orgel L. E.: 1986, *Nature* **321**, 790–792.
Atkinson, D. E.: 1977, *Cellular Energy Metabolism and its Regulation*, Academic Press, Inc., London.
Baltscheffsky, H., Lundin, M., Luxemburg, C., Nyrén, P., and Baltscheffsky, M.: 1986, *Chem. Scr.* **26B**, 259–262.
Bernal, J. D.: 1951, *The Physical Basis of Life*, Routledge and Kegan Paul, London.
Boyer, P. D. and Bryan, D. M.: 1967, in *Methods in Enzymology*, Eastabrook, R. W. and Pullman, M. E. (eds.), Academic Press, vol. 10, pp. 60–71.
Brown, W. E., Smith, J. P., Lehr, J. R. and Frazier, A. W.: 1962, *Nature* **196**, 1050–1054.
Burton, F. G., Neuman, M. W., and Neuman, W. F.: 1969, *Curr. Mod. Biol.* **3**, 20–26.
Cairns-Smith, A. G.: 1982, *Genetic Takeover and the Mineral Origins of Life*, Cambridge University Press, London.
Cairns-Smith, A. G. and Davis, C. J.: 1977, in *The Encyclopaedia of Ignorance: Life Science and Earth Science*, Ducan, R. and Weston-Smith, M. (eds.), Pergamon Press, Oxford, pp. 391–404.
Chan, S., Orenberg, J., and Lahav, N.: 1987, *Origins Life Evol. Biosphere* **17**, 121–134.
de Meis, L.: 1993, *Arch. Biochem. Biophys.* **306**, 287–296.
Erskelens, J.: 1990, *Naturwissenschaften* **77**, 86–87.
Ferris, J. P.: 1968, *Science* **161**, 53–54.
Ferris, J. P. and Hagan, Jr., W. J.: 1984, *Tetrahedron* **40**, 1093–1120.
Ferris, J. P. and Hagan, Jr., W. J.: 1986, *Origins Life Evol. Biosphere* **17**, 69–84.
Ferris, J. P., Huang, C-H., and Hagan, Jr., W. J.: 1988, *Origins Life Evol. Biosphere* **18**, 121–133.
Ferris, J. P., Ertem, G. and Agarwal, V. K.: 1989, *Origins Life Evol. Biosphere* **19**, 153–164.
Fiske, C. H. and SubbaRow, Y.: 1925, *J. Biol. Chem.* **66**, 375–400.
Flodgaard, H. and Fleron, P.: 1974, *J. Biol. Chem.* **249**, 3565–3474.
Gibbs, D., Lohrmann, R., and Orgel, L. E.: 1980, *J. Mol. Evol.* **15**, 347–354.
Hermes-Lima, M.: 1990, *J. Mol. Evol.* **31**, 353–358.
Hermes-Lima, M. and Vieyra, A.: 1989, *Origins Life Evol. Biosphere* **19**, 143–152.
Hermes-Lima, M. and Vieyra, A.: 1992, *J. Mol. Evol.* **35**, 277–285.
Hermes-Lima, M., Tessis, A.C., and Vieyra, A.: 1990, *Origins Life Evol. Biosphere* **20**, 27–41.
Hulshof, J. and Ponnamperuma, C.: 1976, *Origins of Life* **7**, 197– 224.
Jencks, W. P.: 1969, *Catalysis in Chemistry and Enzymology*, McGraw-Hill, Inc., New York, pp. 40–41.
Kulaev, I. S., Mansurova, S. E., Burlakova, E. B., and Dukhovich, V. F.: 1980, *BioSystems* **12**, 177–180.
Lahav, N. and Chang, S.: 1976, *J. Mol. Evol.* **8**, 357–380.
Lahav, N. and Chang, S.: 1982, *J. Mol. Evol.* **19**, 36–45.
Lahav, N., White, D., and Chang, S.: 1978, *Science* **201**, 67–69.
Langmuir, I.: 1918, *J. Amer. Chem. Soc.* **40**, 1361–1403.
Lipmann, F.: 1941, *Adv. Enzymol.* **1**, 99–162.
Lohrmann, R. and Orgel, L. E.: 1971, *Science* **171**, 490–494.
Miller, S. L. and Parris, M.: 1964, *Nature* **204**, 1248–1250.
Morell, S. A. and Bock, R. M.: 1954, Am. Chem. Soc. 126^{th} Meeting, New York, Div. of Biol. Chem. Abstract, 44c.
Neuman, M. W., Neuman, W. F., and Lane, K.: 1970, *Curr. Mod. Biol.* **3**, 277–283.

Orenberg, J. B., Chan, S., Calderon, C., and Lahav, N.: 1985, *Origins Life Evol. Biosphere* **15**, 121–129.
Orgel, L. E.: 1973, *The Origins of Life: Molecules and Natural Selection*, John Wiley & Sons, Inc., New York.
Orgel, L. E.: 1992, *Nature* **358**, 203–209.
Oró, J.: 1976, in *Reflexions on Biochemistry*, Kornberg, A., Cornudella, L., Horecker, B. L., and Oró, J. (eds.), Pergamon Press, New York.
Parker, A. J.: 1961, *J. Chem. Soc.* **83**, 1328–1337.
Parker, A. J.: 1962, *Quart. Rev.* **16**, 163–187.
Pedersen, P. L. and Carafoli, E.: 1987, *Trends Biochem. Sci.* **12**, 186–189.
Pickart, C. M. and Jencks, W. P.: 1984, *J. Biol. Chem.* **259**, 1629–1641.
Plaçon, A. and Tchoubar, C.: 1977, *Clays and Clay Minerals* **25**, 436–450.
Ponnamperuma, C. and Mack, R.: 1965, *Science* **148**, 1221–1223.
Ponnamperuma, C., Sagan, C., and Mariner, R.: 1963, *Nature* **199**, 222–226.
Ponnamperuma, C., Shimoyama, A., and Friebele, E.: 1982, *Origins Life Evol. Biosphere* **12**, 9–40.
Rao, M., Odom, D. G., and Oró, J.: 1980, *J. Mol. Evol.* **15**, 317–331.
Reynolds, R. C.: 1965, *American Mineralogist* **50**, 990–1001.
Stillinger, F. H. and Wassermann, Z.: 1978, *J. Phys. Chem.* **82**, 929–940.
Taves, D. R.: 1963, *Nature* **200**, 1312–1313.
Travers, F. and Douzou, P.: 1974, *Biochemie* **56**, 509–514.
van Kemenade, M. J. J. M. and Bruyn, P. L.: 1987, *J. Coll. Int. Sci.* **188**, 564–585.
Vieyra, A., Gueiros-Filho, F., Meyer-Fernandes, J. R., Costa-Sarmento, G., and Souza-Barros, F.: 1995, *Origins Life Evol. Biosphere* **25**, 335–349.
Wächtershäuser, G.: 1988, *Microbiol. Rev.* **52**, 452–484.
Yamagata, Y., Kojima, H., Ejiri, K., and Inomata, K.: 1982, *Origins of Life* **12**, 333–337.
Yamagata, Y., Watanabe, H., Saitoh, M., and Namba, T.: 1991, *Nature* **352**, 516–519.